9-15-2020

Indium segregation to the selvedge of In_4Se_3 (001)

Archit Dhingra
University of Nebraska–Lincoln, archit.dhingra@huskers.unl.edu

Zoe G. Marzouk
University of Nebraska–Lincoln

Esha Mishra
University of Nebraska–Lincoln, emishra@huskers.unl.edu

Pavlo V. Galiy
Ivan Franko National University of Lviv

Taras M. Nenchuk
Ivan Franko National University of Lviv

See next page for additional authors

Version of Record: https://www.sciencedirect.com/science/article/pii/S0921452620302969
Manuscript_b6c395511fdf08ea4b2345630b690def

Published in Physica B: Condensed Matter, Volume 593, 15 September 2020, 412280

Indium Segregation to the Selvedge of In_4Se_3 (001)

Archit Dhingra[1], Zoe G. Marzouk[1], Esha Mishra[1], Pavlo V. Galiy[2], Taras M. Nenchuk[2], Peter A. Dowben[1]

[1] Department of Physics and Astronomy, University of Nebraska–Lincoln, Jorgenson Hall, 855 North 16th Street, Lincoln, NE 68588-0299, U. S. A.

[2] Electronics Department, Ivan Franko L'viv National University, L'viv, Ukraine

Abstract

Thermal motion of the surface atoms will lead to a decrease in photoemission intensity, while surface segregation may result in an increase of some photoemission intensities. For In_4Se_3(001), both effects are seen. The Debye–Waller factor plot, based on the temperature dependent X-ray photoemission spectroscopy (XPS) measurements on In_4Se_3(001), suggests an upper bound of 203 ± 6 K for the effective Debye temperature, based on the surface component of the In $3d_{5/2}$ core-level. Indium is found to segregate to selvedge (subsurface region) of the crystal.

Keywords: Debye–Waller factor; In_4Se_3; Debye temperature

1. Introduction

Transition metal trichalcogenides (TMTs), of the form MX_3 (M=Ti, Ta, Zr, Hf, etc.; X= S, Se, TE), are 2D materials consisting of 1D chains that are atomically precise in nature [1-3]. Due to the presence of these 1D chains, as their structural unit, these TMTs can exist without dangling bond defects [2,3], thus drawing increased research interest in the field of low-dimensional materials. Edge defects and disorders, which are suppressed in the MX_3 type TMTs, are prevalent in dichalcogenides of transition metals (TMDs) and graphene-based materials causing some undesired properties (which are electronic in nature) that show up with decreases in the width of the semiconductor channel [4-13]. Whether other TMTs, like In_4Se_3, are of interest and possess the properties suitable for devices at transistor widths in the region of 10 nm depends on the facility with which such materials can be manipulated as a 2D material, and adapted to large scale manufacturing. Among the issues of concern are the possibily of significant influence of phonon scattering on carrier mobility (as was observed for TiS_3 [14]) and their phase stability.

In_4Se_3 is a semiconducting material with a layered structure [15-22]. The intralayer interactions in this system are of the strong ionic-covalent kind, whereas the interlayer interactions are of the weaker kind. This system's (001) surface is found to be corrugated (and not smooth) [15], which results in structures having quasi-1D chains at the semiconducting surface of In_4Se_3 (001) system. Additionally, this system is proven to have a band structure that is extremely anisotropic in nature [16–18]; and is found to be dominated by multivalent indium [$(In_3)^{5+}$] bonded with selenium through covalent-ionic bonds. Furthermore, its band gap – which is of the direct kind – is comparable to that of silicon's (1.1 eV) as it lies between a value of 1.1 to 1.3 eV [14–16]. However, the transport measurements dictate that the band gap is about 0.6 eV [18]. Valence band is discovered to be placed well below the Fermi level, as is evident from

the angle resolved valence band photoemission spectroscopy data [15–17,19]. Thus, it is suggested that $In_4Se_3(001)$ is an n-type semiconductor, making it consistent with the transistor measurements [20]. Moreover, the thermoelectric properties possessed by this system make it quite interesting [23–30]. Other non-layered indium selenides have also been investigated for thermoelectric properties [31-35].

A recent study [20] indicated that the $In_4Se_3(001)$ surface terminates in In (as opposed to Se), which differed from the expected results of ground state density functional theory calculations. The possibility of In segregation was, however, by no means excluded in that study. Here, we probe the surface composition further and the effect of thermal motion at the $In_4Se_3(001)$ surface. We have used temperature dependent X-ray photoemission spectroscopy (XPS) in order to investigate the effective Debye temperature (which is one of the key descriptive parameters for the dynamic motion of the atoms) of the core-level In $3d_{5/2}$ component at the system's surface.

2. Experimental Methods

The In_4Se_3 crystals were grown using Czochralski method [15-19]. The (001) crystals are easily cleaved to obtain clean (001) surfaces, as the In_4Se_3 crystal structure is layered [15-22]. The $In_4Se_3(001)$ crystals are single-phased and pure with the lattice constants matching the literature values of a = 15.290 Å, b = 12.307 Å, c = 4.081 Å, while the volume of the elementary cell V = 767.88(4) $Å^3$ [21-22]. The cleaved crystals were examined using X-ray photoemission (XPS).

The core level XPS measurements were carried out using a SPECS X-ray Al anode (hv = 1486.6 eV) source and a hemispherical electron analyzer (PHI Model: 10-360) that has an

angular acceptance of ± 10º or more. All the measurements were performed under ultra-high vacuum (UHV). Samples were cooled between 240–300 K using a liquid nitrogen cryostat connected to the sample holder, as described in [36].

3. Results and discussion

As discussed elsewhere [20], the XPS core level features for the In $3d_{5/2}$ contain two components at 445.4±0.1 eV, and 444.5±0.1 eV. These two In $3d_{5/2}$ core level photoemission features may be attributed to a shift in the surface-to-bulk core level binding energy [20]. These two components are indicated by the fittings to the photoemission core level features, as show in Figure 1. Figure 1 shows there is a decrease in XPS intensity of the surface In $3d_{5/2}$ core-level (at 445.4±0.1 eV) with increasing temperature (from 240–300 K). This change in intensity for the surface In $3d_{5/2}$ core-level (at 445.4±0.1 eV) has been plotted in Fig. 2a. The XPS intensity of the In $3d_{5/2}$ core-level at a binding energy of 444.5±0.1 eV, associated with the bulk of $In_4Se_3(001)$, was found to increase with increasing temperature (see Figures 1 and 2a). An increase in core level intensity, with increasing temperature, suggests an increase in the In concentration. Because this does not occur in the surface component, of the $3d_{5/2}$ core level, the segregation of indium must not be to the surface but to the near surface region, i.e. the selvedge layer or subsurface region. There is no significant change in low energy electron diffraction (LEED) over this range [37], so loss of indium from the surface leading to surface defects is unlikely. The bulk of the crystal is a significant reservoir for In, and we cannot preclude the possibility that the solubility for indium in the selvedge region changes with temperature.

The decrease of intensity of the surface $3d_{5/2}$ core level could be, however, the result of large vibrational amplitudes of the In atoms at the surface. A key parameter for description of

thermal motion of surface atoms perpendicular to the crystal surface and parallel to the scattering vector (Δk) is Debye–Waller scattering, characterized by an effective Debye temperature. The intensity of ejected electrons during XPS is then found to be an exponentially decaying function of absolute temperature, and it can be expressed as [36,38-39]:

$$I = I_0 e^{-2W(T)}$$

Here, $W(T)$ is the Debye–Waller factor and T is the absolute temperature of the system. For a process involving elastic scattering, $W(T)$ can be expressed as [36-45]:

$$W(T) = \frac{3(\hbar\Delta k)^2 T}{2mk_B{\theta_D}^2}$$

As seen in Figure 2b, the intensity of the surface In $3d_{5/2}$ core-level (at 445.4±0.1 eV) photoemission feature follows the Debye–Waller model, unlike the bulk or selvedge In $3d_{5/2}$ core-level component (at a binding energy of 444.5±0.1 eV). The effective Debye temperature of 203 ± 6 K for the surface In $3d_{5/2}$ core-level, can be extracted from the linear fitting in Figure 2b. Since this measurement does not include the in-plane or anharmonic motions, this Debye temperature is only an effective Debye temperature and not the true Debye temperature. This value is significantly less than the effective Debye temperature of 377±20 K, extracted from temperature dependent LEED measurements in this temperature range [37]. The results are, nonetheless, consistent as the LEED is not perfectly surface sensitive and would have some subsurface contribution.

Because segregation of In to the subsurface or selvedge layer is indicated, from the bulk, the effective Debye temperature of 203±6 K for the surface In $3d_{5/2}$ core-level component can only be an upper bound, but the low value is consistent with a layered system with weaker binding between layers.

4. Conclusion

In conclusion, the temperature dependent XPS measurements suggest that the In atoms on the surface of $In_4Se_3(001)$ follow the Debye–Waller model while the In atoms in subsurface region do not. This violation of the Debye–Waller model [36-42], represented by increase in the surface component of the In $3d_{5/2}$ core-level XPS intensity with increasing temperature, implies that In segregates to the selvedge. Therefore, the extracted effective Debye temperature of 203 ± 6 K for the surface In $3d_{5/2}$ core-level can only be an upper bound. These findings suggest phonon scattering may affect transport by reducing carrier mobility. There is now some reason to believe that the solubility of In in the subsurface region of $In_4Se_3(001)$ may be temperature dependent.

Acknowledgments

This research was supported by the National Science Foundation (NSF), through grants NSF-ECCS 1740136, as well as by the nCORE, a wholly owned subsidiary of the Semiconductor Research Corporation (SRC), through the Center on Antiferromagnetic Magneto-electric Memory and Logic task #2760.002. Zoe G. Marzouk was funded through the Nebraska Materials Research Science and Engineering Center (MRSEC) Grant No. DMR-1420645.

References

[1] A. Lipatov, M.J. Loes, H. Lu, J. Dai, P. Patoka, N.S. Vorobeva, D.S. Muratov, G. Ulrich, B. Kästner, A. Hoehl, G. Ulm, X.C. Zeng, E. Rühl, A. Gruverman, P.A. Dowben, A. Sinitskii, ACS Nano 12 (2018) 12713–20. https://doi.org/10.1021/acsnano.8b07703

[2] T.A. Empante, A. Martinez, M. Wurch, Y. Zhu, A.K. Geremew, K. Yamaguchi, M. Isarraraz, S. Rumyantsev, E.J. Reed, A.A. Balandin, L. Bartels, Nano Lett. 19 (2019)

4355-4361. https://doi.org/10.1021/acs.nanolett.9b00958

[3] A. Geremew, M.A. Bloodgood, E. Aytan, B.W.K. Woo, S.R. Corber, G. Liu, K. Bozhilov, T.T. Salguero, S. Rumyantsev, M.P. Rao, A.A. Balandin, IEEE Electronic Device Lett. 39 (2018) 735-738. https://doi.org/10.1109/LED.2018.2820140

[4] S.M.M. Dubois, A. Lopez-Bezanilla, A. Cresti, F. Triozon, B. Biel, J.C. Charlier, S. Roche, ACS Nano 4 (2010) 1971–6. https://doi.org/10.1021/nn100028q

[5] S.A. Jensen, R. Ulbricht, A. Narita, X. Feng, K. Müllen, T. Hertel, D. Turchinovich, M. Bonn, Nano Lett. 13 (2013) 5925–30. https://doi.org/10.1021/nl402978s

[6] M.Y. Han, J.C. Brant, P. Kim, Phys. Rev. Lett. 104 (2010) 056801. https://doi.org/10.1103/PhysRevLett.104.056801

[7] Y.J. Shi, J. Lan, E.J. Ye, W.Q. Sui, X. Zhao, Eur. Phys. J. B. 87 (2014) 251. https://doi.org/10.1140/epjb/e2014-50321-0

[8] Y. Yang, R. Murali, IEEE Electron. Dev. Lett. 31 (2010) 237. https://doi.org/10.1109/LED.2009.2039915

[9] J. Baringhaus, M. Ruan, F. Edler, A. Tejeda, M. Sicot, A. Taleb-Ibrahimi, A.P. Li, Z. Jiang, E.H. Conrad, C. Berger, C. Tegenkamp, W.A. de Heer, Nature 506 (2014) 349–54. https://doi.org/10.1038/nature12952

[10] M. Wimmer, I. Adagideli, S. Berber, D. Tomanek, K. Richter, Phys. Rev. Lett. 100 (2008) 3–6. https://doi.org/10.1103/PhysRevLett.100.177207

[11] V.K. Dugaev, M.I. Katsnelson, Phys. Rev. B. 88 (2013) 235432. https://doi.org/10.1103/PhysRevB.88.235432

[12] E.R. Mucciolo, C.H. Lewenkopf, J. Phys. Condens. Mat. 22 (2010) 273201. https://doi.org./10.1088/0953-8984/22/27/273201

[13] J. Wurm, K. Richter, İ. Adagideli, Phys. Rev. B. 84 (2011) 075468. https://doi.org/10.1103/PhysRevB.84.205421

[14] M. Randle, A. Lipatov, A. Kumar, C.-P. Kwan, J. Nathawat, B. Barut, S. Yin, K. He, N. Arabchigavkani, R. Dixit, T. Komesu, J. Avila, M. C. Asensio, P. A. Dowben, A. Sinitskii, U. Singisetti, J. P. Bird, ACS Nano 13 (2019) 803−811. https://doi.org/10.1021/acsnano.8b08260

[15] Y.B. Losovyj, M. Klinke, E. Cai, I. Rodriguez, J. Zhang, L. Makinistian, A.G. Petukhov, E.A. Albanesi, P.V. Galiy, Ya. Fiyala, J. Liu, P.A. Dowben, Appl. Phys. Lett. 92 (2008) 122107. https://doi.org/10.1063/1.2894577

[16] Y.B. Losovyj, L. Makinistian, E.A. Albanesi, A.G. Petukhov, J. Liu, P.V. Galiy, O.R. Dveriy, P.A. Dowben, J. Appl. Phys. 104 (2008) 083713. https://doi.org/10.1063/1.3000453

[17] K. Fukutani, Y. Miyata, I. Matsuzaki, P.V. Galiy, P.A. Dowben, T. Sato, T. Takahashi, J. Phys. Soc. Jpn. 84 (2015) 1–6. https://doi.org/10.7566/JPSJ.84.074710

[18] D.M. Bercha, O.B. Mitin, L. Yu Kharkhalis, A.I. Bercha, Phys. Solid State 37 (1995) 1778-81.

[19] K. Fukutani, T. Sato, P.V. Galiy, K. Sugawara, T. Takahashi, Phys. Rev. B. 93 (2016) 205156. https://doi.org/10.1103/PhysRevB.93.205156

[20] A. Dhingra, P.V. Galiy, L. Wang et al., Semicond. Sci. Technol. (2020) in press https://doi.org/10.1088/1361-6641/ab7e45

[21] J.H.C. Hogg, H.H. Sutherland, D.J. Williams, Acta Cryst. B. 29 (1973) 1590–3. https://doi.org/10.1107/S056774087300510

[22] A. Likfomann, J. Eitienne, C. R. Acad. Sci. C. 275 (1972) 1097.

[23] J.S. Rhyee, K.H Lee, S.M. Lee, E. Cho, S.Il Kim, E. Lee, Y.S. Kwon, J.H. Shim, G. Kotliar, Nature 459 (2009) 965–8. https://doi.org/10.1038/nature08088

[24] X. Shi, J.Y. Cho, J.R. Salvador, J. Yang, H. Wang, Appl. Phys. Lett. 96 (2010) 162108. https://doi.org/10.1063/1.3389494

[25] J.S. Rhyee, K. Ahn, K.H. Lee, H.S. Ji, J.H. Shim, Adv. Mater. 23 (2011) 2191–4. https://doi.org/10.1002/adma.201004739

[26] G.H. Zhu, Y.C. Lan, H. Wang, G. Joshi, Q. Hao, G. Chen, Z.F. Ren, Phys. Rev. B 83 (2011) 3–6. https://doi.org/10.1103/PhysRevB.83.115201

[27] Y.S. Lim, J.Y. Cho, J.K. Lee, S.M. Choi, K.H. Kim, W.S. Seo, H.H. Park, Electron. Mater. Lett. 6 (2010) 117–21. https://doi.org/10.3365/eml.2010.09.117

[28] J.S. Rhyee, E. Cho, K.H. Lee, S.M. Lee, S. Il Kim, H.-S. Kim, Y.S. Kwon, S.J. Kim, Appl. Phys. Lett. 95 (2009) 212106. https://doi.org/10.1063/1.3266579

[29] X. Yin, J.-Y. Liu, L. Chen, L.-M. Wu, Acc. Chem. Res. 51 (2018) 240–7. https://doi.org/10.1021/acs.accounts.7b00480

[30] Y.-C. Chen, H. Lin, L.-M. Wu, Inorg. Chem. Front. 3 (2016) 1566–71. https://doi.org/10.1039/C6QI00340K

[31] L. Salik, A. Bouhemadou, K. Boudiaf, F. S. Saoud, S. B. Omran, R. Khenata, Y. A. Douri, A.H. Reshak, J. Supercond. Nov. Magn. 33 (2020) 1091–1102. https://doi.org/10.1007/s10948-019-05331-1

[32] X. Y. Shi, F. Q. Huang, M. L. Liu, and L. D. Chen, Appl. Phys. Lett. 94, 122103–122105 (2009). https://doi.org/10.1063/1.3103604

[33] R. Liu, L. Xi, H. Liu, X. Shi, W. Zhang L. Chen, ChemComm. 48 (2012) 3818-3820. https://doi.org/10.1039/c2cc30318c

[34] X. Shen, B. Zhang, Q. Chen, H. Tan, X. Zhang, G. Wang, X. Lu, X. Zhou, Inorg. Chem. Front. 6 (2019) 3545-3553. https://doi.org/10.1039/C9QI01054H

[35] S. Pan, C. Wang, Q. Zhang, B. Yang, Y. Cao, L. Liu, Y. Jiang, L. You, K. Guo, J. Zhang, J. Yang, J. Luo, W. Zhang, ACS Appl. Energy Mater. 2 (2019) 8956-8965. https://doi.org/10.1021/acsaem.9b02004

[36] P. E. Evans, M. Pink, A. A. Zhumekenov, G. Hao, Y. Losovyj, O. M. Bakr, P. A. Dowben, A.J. Yost, J. Phys. Chem. C. 122 (2018) 25506–25514. https://doi.org/10.1021/acs.jpcc.8b08994

[37] P. V. Galiy, Ya. B. Losovyj, T. M. Nenchuk, I. R. Yarovets, Ukr. J. Phys. 59 (2014) 612-621. https://doi.org/10.15407/ujpe59.06.0612

[38] C. Waldfried, D.N. McIlroy, J. Zhang, P.A. Dowben, G.A. Katrich, E.W. Plummer E, Surf. Sci. 363 (1996) 296–302. https://doi.org/10.1016/0039-6028(96)00151-3

[39] C. N. Borca, D. Ristoiu, T. Komesu, H.-K. Jeong, Ch. Hordequin, J. Pierre, J. P. Nozieres, and P. A. Dowben, Appl. Phys. Lett. 77 (2000) 88-90. https://doi.org/10.1063/1.126886

[40] H.K. Jeong, T. Komesu, P.A. Dowben, B.D. Schultz, C.J. Palmstrøm, Phys. Lett. A 302 (2002) 217–223. https://doi.org/10.1016/S0375-9601(02)01048-4

[41] M. A. Van Hove, W.H. Weinberg, C.M. Chan in: Low-Energy Electron Diffraction, (Springer Series in Surface Science, vol. 6, 1986) pp.134

[42] L. J. Clarke, Surface Crystallography, (Wiley, New York, 1985)

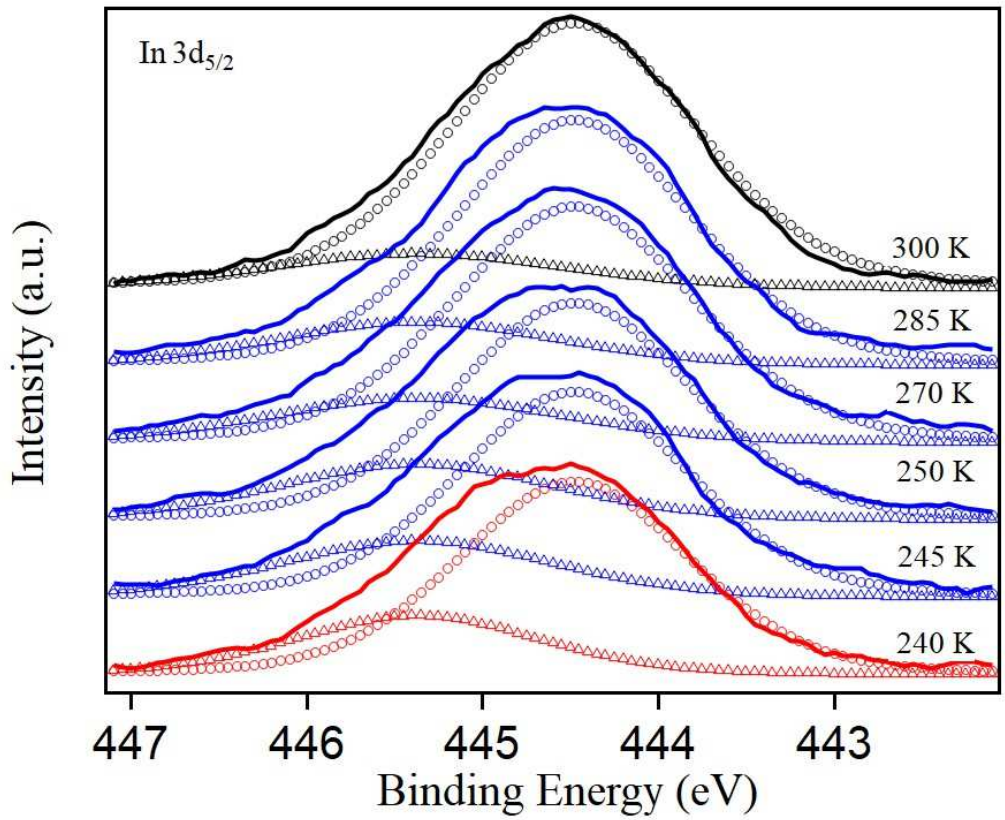

Figure 1. The photoemission spectra of the In $3d_{5/2}$ core-level, with the surface and bulk component indicated. The X-ray photoemission spectra were taken at temperatures between 240 and 300 K. Solid lines represent raw spectra, whereas triangles represent In $3d_{5/2}$ surface core-level component and circles indicate In $3d_{5/2}$ selvedge/bulk core-level component.

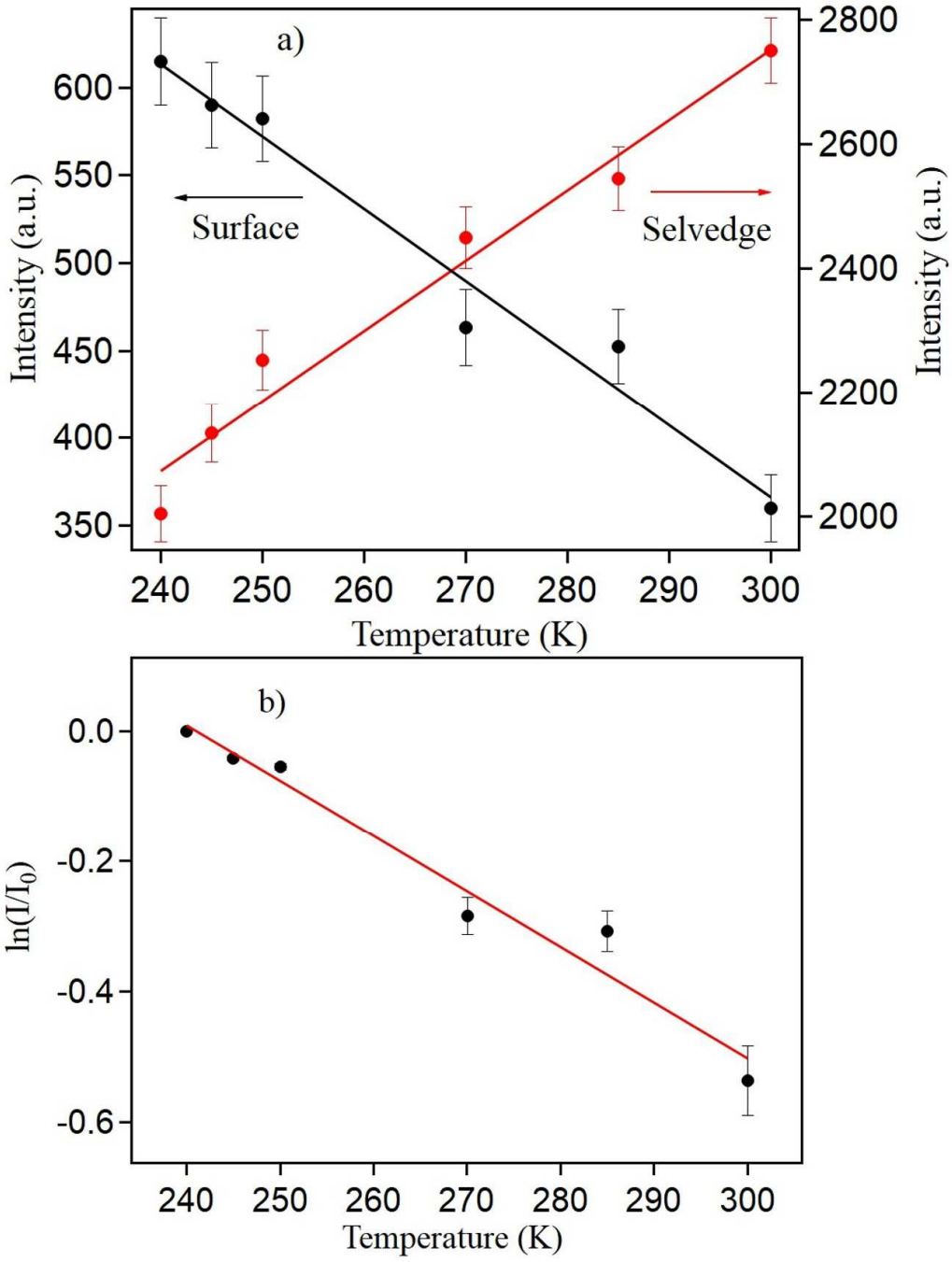

Figure 2. a) The intensity temperature dependence of surface In $3d_{5/2}$ XPS core-level component (black) and selvedge/bulk In $3d_{5/2}$ XPS core-level feature (red) through the temperature range from 240–300 K. b) Debye–Waller factor plot ($\ln(I/I_0)$ vs Temperature) for surface In $3d_{5/2}$ XPS core-level. The upper bound on the effective Debye temperature of 203 ± 6 K is indicated by the linear fit.